

# Paramagnetic Species in Ion Implanted Phosphate Glasses

L. D. BOGOMOLOVA

Institute of Nuclear Physics, Moscow State University, 119992 Moscow, Russia, bogom@mail.com

## Abstract

By means of EPR and optical spectroscopy were investigated phosphate glasses in the system  $x\text{CaO}-(100-x)\text{P}_2\text{O}_5$ , where  $37 \leq x \leq 57$ , implanted with  $\text{Ti}^+$ ,  $\text{Cr}^+$ ,  $\text{V}^+$ ,  $\text{Co}^+$  and  $\text{Mo}^+$  ( $E = 150 \text{ keV}$ , fluences  $F=2 \times 10^{16} \div 5 \times 10^{17} \text{ cm}^{-2}$ ). The EPR spectra of samples co-implanted with  $\text{V}^+$  and  $\text{O}^+$  as well as  $\text{Mo}^+$  and  $\text{O}^+$  were also studied. Some samples were co-implanted with  $^{95}\text{Mo}^+$  and  $\text{O}^+$ . EPR spectra were recorded at room temperature, 77K, in the range from 100 to 450K and at 4.2K. The results are discussed together with data obtained earlier in our laboratory for phosphate glasses implanted with transition metals (TM). It is shown that the ions of transition metals  $\text{Ti}^{3+}$ ,  $\text{V}^{3+}$ ,  $\text{V}^{4+}$ ,  $\text{Cr}^{3+}$ ,  $\text{Mn}^{2+}$ ,  $\text{Co}^{2+}$ ,  $\text{Cu}^{2+}$ ,  $\text{Mo}^{5+}$  can be present in isolated states in implantation layers of phosphate glasses at a rather low fluences ( $\leq 5 \times 10^{16} \text{ cm}^{-2}$ ). The ions in high valences forms ( $\text{V}^{4+}$ ,  $\text{Mo}^{5+}$ ) are formed only in the case of co-implantation with  $\text{O}^+$ . The ions  $\text{Ti}^{3+}$ ,  $\text{V}^{4+}$ ,  $\text{Mo}^{5+}$  are in tetragonally compressed octahedral and Ion  $\text{Cu}^{2+}$  is in tetragonally elongated octahedron, i.e. are in their the most typical environments. However, spectral parameters for these ions differ from those obtained for them in glasses of corresponding compositions melted from the batch. The isolated ions  $\text{Cr}^{3+}$  and  $\text{Co}^{2+}$  are in octahedral coordination. At high fluences ( $\geq 10^{17} \text{ cm}^{-2}$ ) some TM ions can form in implanted phosphate glasses compounds with O or PO groups (for example, antiferromagnetic crystals MnO, compounds with phase transition at 340K  $\text{VO}_2$ , ferromagnetic crystals  $\text{CrO}_2$  with temperature Curie,  $T_c = 390\text{K}$ , non-stoichiometric compound  $\text{Ti}_x\text{PO}_4$ ).

## INTRODUCTION

Electron paramagnetic resonance (EPR) yields information concerning valence state and local environment of implanted transition metal (TM) ions, as well as the nature of structural defects induced in the substrate by the implantation. EPR is also very sensitive to interactions among transition ions, and to the formation of both clusters and fine crystalline inclusions containing atoms of transition metals.

It is known that ion implantation may induce changes in physical and chemical properties of near-surface layers of glasses [1]. Modification of optical, magnetic and electrical properties of these layers is expected in the case of implantation of TM with partially filled d-electron shells. EPR is effectively applied to the study of silica glasses implanted with TM ions. [2-8] this attention is due to practicable interest connected with formation of colloidal metallic nanometer-sized clusters, which exhibit particular optical and magnetic properties, and are promising candidates for application in integrated optics.

To our knowledge, EPR spectra of TM ions implanted into oxide glasses of more complex compositions were studied a little. At the same time paramagnetic structural defects induced by ion implantation in oxide glasses, including phosphate glasses, have been studied [9-13]. We investigated structural defects in many components and some binary phosphate glasses implanted with  $\text{C}^+$ ,  $\text{N}^+$ ,  $\text{O}^+$ ,  $\text{Ar}^+$ ,  $\text{Mn}^+$ ,  $\text{Cu}^+$  and  $\text{Pb}^+$  under different conditions [9-13]. It has been found that in

all the phosphate glasses for all implants the molecular  $O_2^-$  ions weakly coupled with glass-network were formed [9-13]. For glasses containing  $P_2O_5 \leq 50$  mol.% implanted with  $N^+$  EPR spectrum of  $NO_2$  has been obtained [11]. The molecular  $CO_2^-$  ions are formed in phosphate glasses implanted with  $C^+$  [12]. For all phosphate glasses implanted with  $Pb^+$  the narrow line at  $g=1.9986$  which was observed neither other glasses nor other implants has been found [12].

This paper aims to study phosphate glasses implanted with TM by means of EPR. We would like to obtain information concerning the peculiarities of the incorporation of implanted TM into phosphate substrate.

EPR spectra of  $Mn^{2+}$  and  $Cu^{2+}$  in some phosphate glasses have been presented in our earlier work [9]. Structureless line of  $Cu^{2+}$  with  $g_{||} = 2.26$  and  $g_{\perp} = 2.05$  was observed in  $Cu^+$  - implanted phosphate glasses. The well resolved hyperfine structure (HFS) of  $Mn^{2+}$  ions with HFS constant  $A \sim 8mT$  at  $g=2$  has been found in some phosphate glasses implanted with  $Mn^+$  [9] at low fluences of implanted ions. At higher fluences ( $F > 10^{17} cm^{-2}$ ) the crystalline antiferromagnetic compounds  $MnO$  are formed. Recently [14] we investigated phosphate glasses implanted with  $Ti^+$ ,  $V^+$ ,  $Co^+$ . In Ref [14] glasses of composition (in mol.%):  $65P_2O_5 - 10B_2O_3 - 10 Al_2O_3 - 15 MgO$  (denoted as P-13) have been studied. The glasses of this composition have been chosen as a material used for radioactive waste encapsulation, and structural paramagnetic defects in these glasses have been studied earlier [9-12].

As shown [14] in P-13 glass implanted with  $Ti^+$  at a rather low fluences titanium is present as isolated ions  $Ti^{3+}$  in tetragonally compressed octahedron with  $|xy\rangle$  ground state. At fluences  $F > 10^{17} cm^{-2}$  non-stoichiometric crystalline compound  $Ti_xPO_4$  is formed. In P-13 glass implanted with  $V^+$  to  $F \sim 5 \times 10^{16} cm^{-2}$  vanadium is present mainly in  $V^{3+}$  valence state according to optical data. In the samples co-implanted with  $V^+$  and  $O^+$  EPR spectrum typical of  $V^{4+}$ , appears. In the EPR SPECTRUM of P-13 glass implanted with  $Co^+$  ions the broad line at  $g=4.2$  have been found at temperature of liquid He. The line was attributed to  $Co^{2+}$  in distorted octahedral environment.

In the present work we continue to study EPR spectra of  $V^+$ - and  $Co^+$ - implanted phosphate glasses. In addition, the EPR data for phosphate glasses implanted with  $Cr^+$  and  $Mo^+$  were obtained. We would like to summarize and discuss the data, concerning the incorporation of TM into phosphate glasses, obtained in our laboratory, including Refs. [9,14].

## EXPERIMENTAL

We investigated phosphate glasses of composition P-13 and binary glasses in the system  $x CaO - (100-x)P_2O_5$ , where  $37 \leq x \leq 57$ . The glasses were melted in high-frequency furnace in air atmosphere. Then they were cast and annealed in electric muffle furnace preheated to annealing temperature.

At this temperature the glasses were held for periods from 30 to 60 min and then were cooled to room temperature at rate about 0.5 degrees per min. The polished samples were prepared. Samples size was  $10 \times 20 \times 0.5$  mm. The plates were irradiated at energy  $E=150keV$  with  $Ti^+$  (fluences  $F = 2 \times 10^{16} \div 2 \times 10^{17} cm^{-2}$ ),  $Cr^+$  ( $F=2 \times 10^{16} \div 5 \times 10^{17} cm^{-2}$ ),  $V^+$  ( $F=5 \times 10^{16} \div 5 \times 10^{17} cm^{-2}$ ),  $Co^+$  ( $F=2 \times 10^{16} \div 2 \times 10^{17} cm^{-2}$ ), and  $Mo^+$  ( $F=5 \times 10^{16} \div 2 \times 10^{17} cm^{-2}$ ). The EPR spectra of samples co-implanted with  $V^+$  ( $E=150 keV$ ,  $F=5 \cdot 10^{16} cm^{-2}$ ) and  $O^+$  ( $E=90 keV$  at different fluences) as well as  $Mo^+$  ( $E=150 keV$ ,  $F=5 \cdot 10^{16} cm^{-2}$ ) and  $O^+$  ( $E=90 keV$  at different fluences) were also studied. Some samples were co-implanted with  $^{95}Mo^+$  and  $O^+$ . Rate of fluence  $j=1 \div 0.5 \mu A/cm^2$ .

After implantation the slabs were crushed and used for EPR measurements. EPR measurements were performed using a modified spectrometer RE-1306 (Russian model) and

Bruker-BER-418 operating at X-band frequency. EPR spectra were recorded at room temperature, 77K, in the range from 100 to 450 K and at 4.2K. The absolute concentrations of paramagnetic species were determined with reference to hyperfine transition ( $1/2 \leftrightarrow 1/2$ ) of  $Mn^{2+}$ : MgO or  $CuSO_4 \cdot 5H_2O$  powder samples previously calibrated in Russian Institute of Standards.

Optical spectra for some samples were measured at room temperature with SP-8 spectrophotometer in wavelength region from 300 to 1200 nm.

Concentration and depth profiles of implanted ions were determined from Rutherford backscattering (RBS) ( $2 \text{ MeV He}^+$  ions at scattering angle  $160^\circ$ ).

Spectral EPR parameters of  $V^{4+}$  and  $Mo^{5+}$  ions were obtained by comparison of experimental and simulated spectra. Method of calculation of similar spectra has been described in many of our works (for example, in Ref. [15]).

## RESULTS

As mentioned above, structural defects in ion-implanted phosphate glasses have been studied and discussed in Refs. [9-13]. Here we consider only EPR signals which can be associated with transition metals incorporated into substrates.

The EPR spectrum of the sample P-13 implanted with  $Ti^+$  to fluence  $F=2 \times 10^{16}$  per  $cm^2$  has been presented in Ref. [14]. In the samples of the system  $CaO-P_2O_5$  the single asymmetric line with  $g=1.925 \div 1.933$  at zero-crossing position and width  $\Delta H_{pp}$  depending on glass composition and fluence (see table 1) were observed. The linewidth does not depend on temperature, and the intensity increases with decreasing measurement temperature. As follows from table 1 the broad single line is observed in ultraphosphate and metaphosphate samples implanted to high fluences. The width of this line is  $\Delta H_{pp} = 30 \div 33 \text{ mT}$  at 295 K and  $g=1.940 \pm 0.002$ . The EPR line with  $g=1.92 \div 1.94$  have been observed in many oxide glasses [16-18] including  $Ti^+$  - implanted silica glasses and have been attributed to  $Ti^{3+}$  ions [5,7].

Figure 1 shows temperature dependence of the widths and intensities of the  $g=1.940$  line. It can be seen that both  $\Delta H_{pp}$  and the intensity decrease with decreasing temperature. Similar line has been observed for P-13 [14].

In Figure 2 EPR spectrum of  $45CaO-55 P_2O_5$  sample implanted with  $Cr^+$  at  $F=3 \times 10^{16} \text{ cm}^{-2}$  is shown. As follows from this figure EPR spectrum contains two well known lines: peak at  $g \sim 5.2$  and line with  $g=1.975$ , observed for isolated ions  $Cr^{3+}$  in many oxide glasses [17,19,20]. At higher fluences a single line with  $g \sim 1.97$  was observed (inset in Figure 2, bottom) which can be attributed to  $Cr^{3+}$  clusters coupled by exchange interactions [21].

For the sample  $57CaO-43 P_2O_5$  implanted with  $Cr^+$  to fluence  $F=5 \times 10^{17} \text{ cm}^{-2}$  the almost symmetric line at  $g \sim 1.98$  with width  $\Delta H_{pp} \sim 25 \text{ mT}$  (not shown) was observed at 360K. Below 320 K the low-field shoulder appears and is further shifted to lower fields with decreasing temperature (Inset, Figure 2, top).

As follows from Ref. [14], depth profile of V in the glass P-13 obtained by means of RBS indicates that V enters into implantation layer. However, no EPR spectrum was observed for this sample. The absorption bands at 380, 455 and 720 nm in optical spectrum of this sample are typical of  $V^{3+}$  ions in phosphate glasses [22-24], i.e. some portion of implanted V enters the glass in the  $V^{3+}$  valence state. In the sample firstly implanted with  $V^+$  and then  $O^+$  optical spectrum contains absorption bands typical of  $V^{4+}$  ion and EPR spectrum of  $V^{4+}$  with HFS appears for this sample.

TABLE 1  
EPR data for titanium-implanted calcium-phosphate glasses

Nos	Composition (mol.%)		Name	Fluence, $10^{17} \text{cm}^{-2}$	$\text{Ti}^{3+}$ (iso)		$\text{Ti}_6\text{PO}_4$		Concentr. $\text{Ti}^{3+}_{\text{iso}}, \text{cm}^{-2}$	Ratio $\text{Ti}^{3+}_{\text{iso}}/\text{Ti}_{\text{total}}$
	CaO	$\text{P}_2\text{O}_5$			g	Width, mT	g	Width, mT		
1	37	63	Ca-37	0.2	1.932	11			$6 \times 10^{18}$	30%
2	37	63	Ca-37	0.5	1.931	11			$8 \times 10^{18}$	16%
3	37	63	Ca-37	0.8	1.929	10	1.940	31	$5 \times 10^{18}$	6.25%
4	37	63	Ca-37	2	1.925	10	1.939	32	$4 \times 10^{18}$	2%
5	37	63	Ca-37	5	1.932	9	1.940	34	$2 \times 10^{18}$	0.4%
6	45	55	Ca-45	0.2	1.933	10			$4 \times 10^{18}$	20%
7	45	55	Ca-45	0.5	1.932	11			$7 \times 10^{18}$	14%
8	45	55	Ca-45	0.8	1.931	12			$8 \times 10^{18}$	10%
9	45	55	Ca-45	2	1.928	9	1.939	33	$3 \times 10^{18}$	1.5%
10	45	55	Ca-45	5	1.932	8	1.940	32	$1.6 \times 10^{18}$	0.32%
11	50	50	Ca-50	0.2	1.931	9			$3.6 \times 10^{18}$	16%
12	50	50	Ca-50	0.5	1.925	10			$4.7 \times 10^{18}$	9.4%
13	50	50	Ca-50	0.8	1.933	11			$8 \times 10^{18}$	7.5%
14	50	50	Ca-50	2	1.932	7	1.940	31	$0.6 \times 10^{18}$	0.3%
15	50	50	Ca-50	5	1.931	7	1.939	32	$4 \times 10^{18}$	0.08%
16	57	43	Ca-57	0.2	1.930	10			$4 \times 10^{18}$	20%
17	57	43	Ca-57	0.5	1.928	10			$5 \times 10^{18}$	10%
18	57	43	Ca-57	0.8	1.925	11			$7 \times 10^{18}$	8.75%
19	57	43	Ca-57	2	1.932	7.5			$1.3 \times 10^{18}$	6.5%
20	57	43	Ca-57	5	1.912	7			$2 \times 10^{18}$	4%

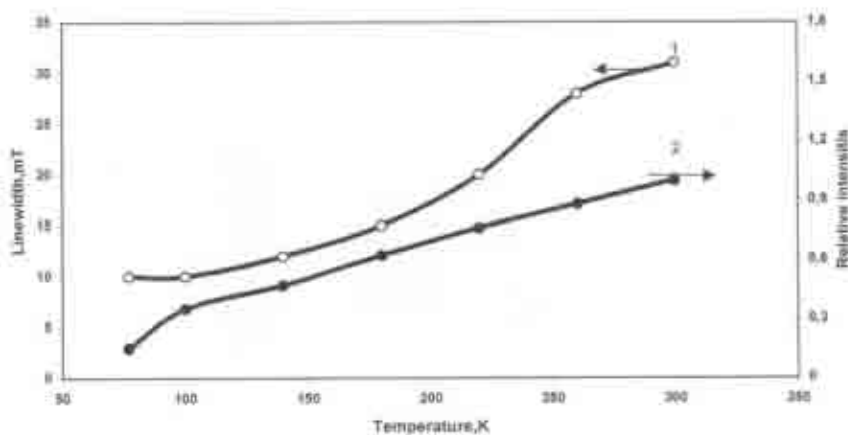


Figure 1: Dependence of width (1) and intensity (2) of the  $g = 1.940$  line on measurement temperature for the sample Ca-37 (see table) implanted with  $Ti^+$  at  $F=5 \times 10^{17} \text{ cm}^{-2}$

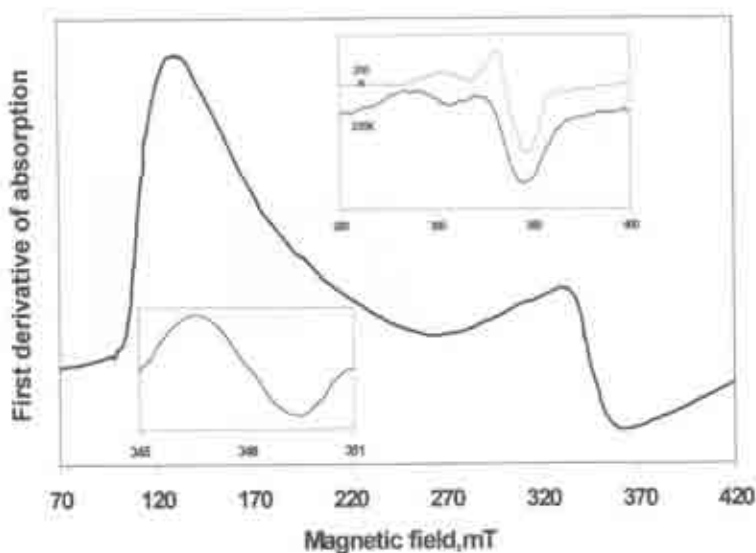
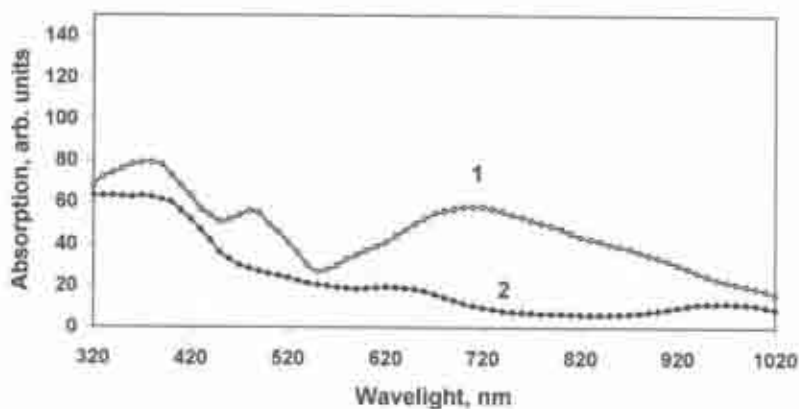


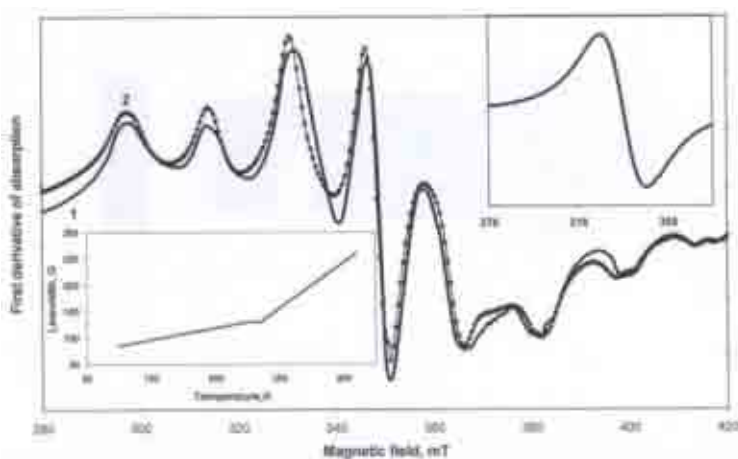
Figure 2: EPR spectrum of the sample  $45CaO-55P_2O_5$  implanted with  $Cr^+$  at  $F=3 \times 10^{16} \text{ cm}^{-2}$ . Inset (top) shows EPR spectrum of the sample  $57CaO-43 P_2O_5$  implanted with  $Cr^+$  at  $F=5 \times 10^{17} \text{ cm}^{-2}$ .

Figure 3 shows optical spectra of the sample  $45CaO-55 P_2O_5$ . The absorption bands (spectrum 1) at 370, 460 and 730 nm are seen. They are typical for  $V^{3+}$  in phosphate glasses [22-24]. No EPR spectrum is observed for this sample. In phosphate glasses  $xCaO-(100-x) P_2O_5$  containing  $>50 \text{ mol.}\%$   $P_2O_5$  implanted with  $V^+$ , vanadium is present mainly in  $V^{3+}$  state according to optical data. This ion is non-kramers and does not give EPR spectra in non-ordered systems. In optical spectrum of glasses with  $x < 50$  (and co-implanted with  $O^+$  at

$F < 1 \times 10^{17} \text{ cm}^{-2}$ ) the broad weak absorption bands (spectrum 2) at  $\sim 640$  and  $\sim 1000 \text{ nm}$  typical of  $V^{4+}$  in phosphate glasses [22-24] are observed, Figure 4 shows experimental (1) and calculated (2) EPR spectrum with HFS of  $V^{4+}$  in the sample  $50\text{CaO}-50 \text{P}_2\text{O}_5$  co-implanted with  $V^+$  ( $F=5 \times 10^{16} \text{ cm}^{-2}$ ) and  $O^+$  ( $F=10^{17} \text{ cm}^{-2}$ ). In glasses containing  $< 50 \text{ mol. P}_2\text{O}_5$  implanted with  $V^+$  to fluences  $F > 1 \times 10^{17} \text{ cm}^{-2}$  the single line at  $g \sim 1.96$  with  $\Delta H_{pp} \sim 13 \div 20 \text{ mT}$  (Figure 4, Inset, top) was observed at room temperature. The width of this line decreases with increasing fluence of  $O^+$ . Temperature dependence of the width of this line (Figure 4, Inset, bottom) indicates phase transition at  $\sim 350\text{K}$ .



**Figure 3:** Optical spectra of the glass  $50\text{CaO}-50 \text{P}_2\text{O}_5$  co-implanted with  $V^+$  at  $F=5 \times 10^{16} \text{ cm}^{-2}$  (spectrum 1) and co-implanted with  $V^+$  at  $F=5 \times 10^{16} \text{ cm}^{-2}$  and  $O^+$  ( $F=10^{17} \text{ cm}^{-2}$ ).



**Figure 4:** EPR spectra of the glass  $50\text{CaO}-50\text{P}_2\text{O}_5$  co-implanted with  $V^+$  at  $F=5 \times 10^{16} \text{ cm}^{-2}$  and  $O^+$  ( $F=10^{17} \text{ cm}^{-2}$ ) (1-experimental, 2-calculated), EPR line at  $g=1.96$  of the sample  $37\text{CaO}-63 \text{P}_2\text{O}_5$  co-implanted with  $V^+$  at  $F=10^{17} \text{ cm}^{-2}$  and  $O^+$  ( $F=2 \times 10^{17} \text{ cm}^{-2}$ ) at room temperature (Inset, top). Temperature dependence of the width of  $g=1.96$  line (inset, bottom)

In Figure 5 is presented EPR spectrum of 45CaO-55 P<sub>2</sub>O<sub>5</sub> glass implanted with Co<sup>+</sup> ( $F=5 \times 10^{16} \text{ cm}^{-2}$ ) which contains the broad ( $\Delta H_{pp} \sim 120 \text{ mT}$ ) asymmetric line with base-crossing  $g \sim 4.2$ . In Figure 5 (Inset, top) is shown the EPR spectrum of the same sample implanted with Co<sup>+</sup> at  $F=8 \times 10^{16} \text{ cm}^{-2}$  which contains less broad ( $\Delta H_{pp} \sim 70 \text{ mT}$ ) and more symmetric line. Inset (bottom) of Fig 5 presents the depth profile of Co for the sample implanted at  $F=5 \times 10^{16} \text{ cm}^{-2}$  measured by means of RBS. The concentration maximum of Co is at 118 nm.

In Figure 6 (Inset, bottom) is shown optical spectrum of the sample 50CaO-50 P<sub>2</sub>O<sub>5</sub> implanted with Mo<sup>+</sup> with natural contents of isotopes implanted to  $F=5 \times 10^{16} \text{ cm}^{-2}$ . This spectrum (1) contains three absorption bands at 370, 450 and 740 nm. No EPR spectrum was observed for this sample. Optical spectra of Mo in phosphate glasses are complex and studied a little. The absorption bands presented in the spectrum 1 are presumably due to valence forms of Mo (Mo<sup>2+</sup> or Mo<sup>4+</sup>) [25]. Co-implantation with O<sup>+</sup> at  $F=10^{17} \text{ cm}^{-2}$  leads to appearance of the EPR spectrum shown in Figure 6 (Inset, top) and broad absorption band with maximum at 720÷730 in optical spectrum (Figure 6, Inset, bottom). This band [25] as well as the EPR spectrum with parameters  $g_{\perp}=1.92$  and  $g_{\parallel}=1.88$  are due to Mo<sup>5+</sup> [26]. Molybdenum in its natural abundant state is composed of seven isotopes, of which some 75% are of even mass number and zero nuclear spin and the remaining 25% of odd mass number and having a nuclear spin of 5/2.

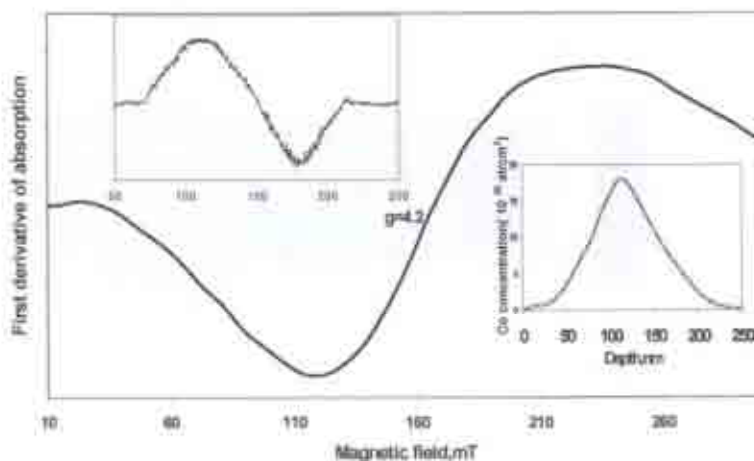


**Figure 5: EPR spectrum of the sample 45CaO-55 P<sub>2</sub>O<sub>5</sub> implanted with Co<sup>+</sup> at  $F=5 \times 10^{16} \text{ cm}^{-2}$ . EPR spectrum of the same sample implanted with Co<sup>+</sup> to  $F=8 \times 10^{16} \text{ cm}^{-2}$  (Inset, top). Depth Co profile obtained by means RBS for the sample 45CaO-55 P<sub>2</sub>O<sub>5</sub> implanted with Co<sup>+</sup> at  $F=5 \times 10^{16} \text{ cm}^{-2}$**

Thus, the spectrum shown in Figure 6 (Inset) is due to Mo with the even mass number isotopes. We investigated EPR spectrum of the sample of the same composition implanted with <sup>95</sup>Mo<sup>+</sup> at fluence  $F=5 \times 10^{16} \text{ cm}^{-2}$  and co-implanted with O<sup>+</sup> at  $F=10^{17} \text{ cm}^{-2}$  shown in Figure 6 (1-experimental, 2- calculated). The spectrum has HFS. The content of Mo<sup>5+</sup> in respect to nominal content of implanted Mo is  $\sim 3,8\%$ . The single line with  $g \sim 1.91$  is observed at higher fluences.

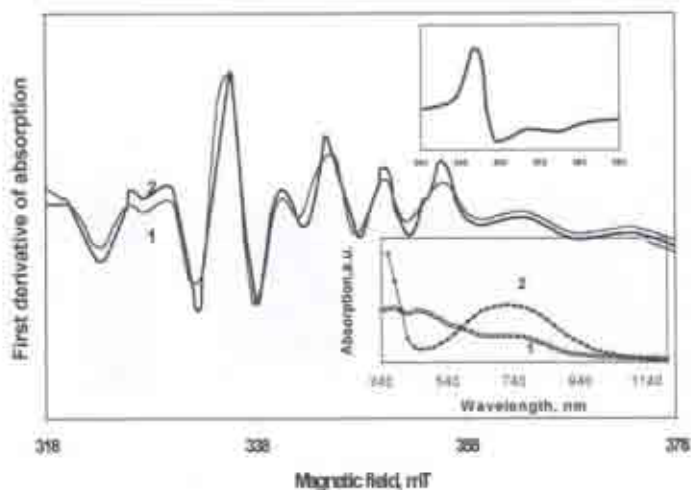


**Figure 6:** EPR spectra of the glass 50CaO-50 P<sub>2</sub>O<sub>5</sub> implanted with <sup>95</sup>Mo+ at  $F=5 \times 10^{16} \text{ cm}^{-2}$  and  $O^+$  ( $F=10^{17} \text{ cm}^{-2}$ ) (1-experimental, 2-calculated), EPR spectrum of the same sample implanted with Mo+ with natural content of isotopes (Inset, top). Optical spectra of the sample 50CaO-50 P<sub>2</sub>O<sub>5</sub> implanted with Mo+ at  $F=5 \times 10^{16} \text{ cm}^{-2}$  (spectrum 1) and co-implanted with Mo+ at  $F=5 \times 10^{16} \text{ cm}^{-2}$  and  $O^+$  ( $F=10^{17} \text{ cm}^{-2}$ )

## DISCUSSION

### Titanium

As mentioned above, in calcium-phosphate glasses implanted with Ti<sup>+</sup> asymmetric EPR lines with  $g=1.925 - 1.933$  are observed. Similar lines have been reported for many oxide glasses doped with Ti and have been attributed to “isolated” Ti<sup>3+</sup> ions (Ti<sup>3+</sup> iso) in compressed octahedral environment with  $|xy\rangle$  ground state [16-18]. As seen in Table 1, concentration of Ti<sup>3+</sup> iso increases with fluence of implanted ions (for example, samples Ca-57, Ca-50(11→13), etc; However, the content of Ti<sup>3+</sup> iso is small (<30%) relative to nominal number of implanted Ti and decreases with increasing fluence. It means that the considerable part of titanium enters in implantation layer in non-paramagnetic state or forms antiferromagnetic pairs  $Ti^{3+} = Ti^{3+}$ . Especially low fraction of Ti<sup>3+</sup> iso is formed in the samples where the second lines (with  $g=1.94$ ) was observed. The last appears mainly in ultra- and metaphosphate glasses at high fluences.

As follows from Figure 1 both  $\Delta H_{pp}$  and the intensity decrease with decreasing temperature for the  $g=1.94$  line. We assume that this line belongs to non-stoichiometric crystalline compound  $Ti_xPO_4$  formed in implantation layer. The line with similar  $g$ -value, width and temperature dependence has been observed in Ref. [27]. Stoichiometric  $TiPO_4$  contains the pairs  $Ti^{3+} = Ti^{3+}$  and is non-paramagnetic. The results are interpreted in terms of the existence of defects in  $TiPO_4$  which favour to the appearance of non-paired Ti<sup>3+</sup> ions contributing to EPR line. Temperature dependence of intensity and which of this line has been explained by recombination of defects with decreasing temperature [27]. Similar line has been observed in Ref. [14], too.

## Chromium

EPR spectra analogous to the spectrum shown in Figure 2 have been reported for many oxide glasses containing Cr and have been attributed to  $\text{Cr}^{3+}$  [1, 19.2.] in octahedral environment. As mentioned above at higher fluences a single line with  $g \sim 1.98$  was observed (Inset in Figure 2, bottom) which according literature data can be attributed to  $\text{Cr}^{3+}$  clusters coupled by exchange interactions [21].

As mentioned above a single line at  $g \sim 1.98$  with  $\Delta H_{pp} \sim 25$  mT is observed for the sample 57 CaO-43 PO implanted with  $\text{Cr}^{3+}$  to fluence  $F = 5 \times 10^{17} \text{ cm}^{-2}$  at 360 K. The shape of this line depends strongly on temperature (Figure 2, Inset, top). The shape of this line becomes asymmetric and low-field shoulders appear. Similar behavior is typical of ferromagnetic resonance (FMR).

It has been shown [29] that the shape and width of FMR line associated with a random ensemble of ferromagnetic particles dispersed in the medium is almost always determined by magnetocrystalline anisotropy. The temperature dependence of FMP line has been ascribed to the temperature dependence of anisotropy field  $H_a$  [29]. Experimental linewidth is a crude measure of anisotropy field  $H_a$ .

It is known that among chromium oxides only  $\text{CrO}_2$  is a ferromagnetic at room temperature (below its Curie temperature  $T_0 \cong 390$  K) [30]. FMR investigations of  $\text{CrO}_2$  supported on  $\text{TiO}_2$  are reported in Ref. [31]. It has been shown that in tetragonal  $\text{CrO}_2$  magnetocrystalline anisotropy is axial. The temperature dependence of the shape of FMR line shown in Figure 4 is similar to that observed in Ref [30].

## Vanadium

As mentioned above, in P-13 glass implanted with  $\text{V}^{3+}$  vanadium is present mainly in  $\text{V}^{3+}$  state. In the case of co-implantation  $\text{V}^{3+}$  and  $\text{O}^+$  the optical bands typical of  $\text{V}^{4+}$  ions appear and EPR spectrum of  $\text{V}^{4+}$  is observed. This spectrum is described by spin-Hamiltonian of an axial symmetry with electron spin  $S = 1/2$  and nuclear spin  $I = 5/2$ .

$$H = g_{\parallel} \beta H_z S_z + g_{\perp} \beta (H_x S_x + H_y S_y) + A_{\parallel} S_z I_z + A_{\perp} (S_x I_x + S_y I_y) \quad (1)$$

The symbols are standard.

The comparison of experimental and calculated spectra for the glass P-14 shows that the best-fit parameters of spin-Hamiltonian are  $g_{\parallel} = 1.936 \pm 0.002$ ;  $g_{\perp} = 1.973 \pm 0.002$ ;  $A_{\parallel} = (170 \pm 2) 10^{-4} \text{ cm}^{-1}$   $A_{\perp} = (62 \pm 3) 10^{-4} \text{ cm}^{-1}$ . From these spectra parameters follows that  $\text{V}^{4+}$  ions are located in tetragonally compressed octahedron of  $C_{4v}$  symmetry. It should be emphasized that  $\text{V}^{4+}$  ions are formed only as the result of co-implanted with oxygen.

In calcium-phosphate glasses of ultraphosphate compositions vanadium is present in  $\text{V}^{3+}$  form giving optical absorption bands shown in Figure 3 (spectrum 1). No EPR spectra were observed for these glasses. In glasses containing  $\leq 50$  mol. %  $\text{P}_2\text{O}_5$  and co-implanted with  $\text{O}^+$  optical absorption bands appear (Figure 3, spectrum 2) and EPR spectrum of  $\text{V}^{4+}$  becomes observable.

Computer simulation of experimental spectrum for the sample metaphosphate composition co-implanted with  $\text{V}^{4+}$  and  $\text{O}^+$  shown in Fig 4 gives the best-fit parameters of spin Hamiltonian (1) are  $g_{\parallel} = 1.925$ ;  $g_{\perp} = 1.97$ ;  $A_{\parallel} = 150 \times 10^{-4} \text{ cm}^{-1}$  and  $A_{\perp} = 44 \times 10^{-4} \text{ cm}^{-1}$ . The relationship between  $g_{\parallel}$  and  $g_{\perp}$  indicates that  $\text{V}^{4+}$  is in compressed octahedron with ground state  $|xy\rangle$ .

It should be noted that obtained parameters differ from those observed for  $\text{V}^{4+}$  in calcium – phosphate glasses of metaphosphate composition prepared by melting of the batch with

addition of  $P_2O_5$  [23,31]. It indicates that although the environment of  $V^{4+}$  in implanted layer is compressed octahedron the last is distinct from one formed during the cooling of the melt.

As mentioned above, in glasses containing <50 mol. %  $P_2O_5$  implanted to fluences  $F > 1 \times 10^{17} \text{ cm}^{-2}$  the single line at  $g \sim 1.96$  with  $\Delta H_{pp} \sim 13 \div 20 \text{ mT}$  was observed at room temperature. The decrease in linewidth with increasing fluence can be explained by narrowing as the result of exchange interaction among  $V^{4+}$  with the growth of implanted vanadium. Temperature dependence of the width of this line (Figure 4, *bottom*) indicates phase transition at  $\sim 350\text{K}$ . It is known that  $VO_2$  crystals exhibit insulator-metal transition at  $\sim 340\text{K}$  EPR spectra of  $V^{4+}$  in  $VO_2$  have been observed when this crystal contains impurities replacing  $V^{4+}$  in antiferromagnetic pairs  $V^{4+} - V^{4+}$ .

## Cobalt

Ion  $Co^{2+}$  with  $d^7$  electron configuration and  $^4F$  ground state has seven fold orbital degeneracy. The  $^4F$  state of  $d^7$  ions in octahedral field splits to  $^4T$  triplet ground state. Spin – orbital interaction leads to splitting of this triplet so that the lowest state is kramers doublet with isotropic  $g = 4.3$ . The fields of lower symmetry mix this state with nearly lying excited states, and  $g$ -value becomes anisotropic [33]. However, its average value remains around  $g=4$  although the observed line becomes broad and smooth. Such a situation takes place in the case of silica glass implanted with  $Co^+$  ions [6]. The  $g \sim 4.2$  (Figure 5) is close to  $g$ -value typical for octahedral environment of  $Co^{2+}$ , and large width of the line indicates the strong distortion of this environment. Because of short spin-lattice time EPR of  $Co^{2+}$  is observed in octahedral coordination only at low temperatures. Measurements by means of optical and infrared spectroscopy showed that in binary  $CoO-P_2O_5$  glasses of ultraphosphate composition cobalt is present as  $Co^{2+}$  in octahedral coordination [33]. The comparison of RBS and EPR data shows that Co enters into implantation layer mainly in  $Co^{2+}$ . It should be noted that few works on EPR  $Co^{2+}$  in oxide glasses as well as in glasses prepared by sol-gel technique have been reported [34-36]. The results obtained in the present paper are in good agreement with these works.

## Molybdenum

As shown in section 4, two kinds of EPR spectra are observed for metaphosphate glasses co-implanted with  $Mo^+$  and  $O^+$ : one of them is an axial spectrum with  $g_{\perp} = 1.92$  and  $g_{\parallel} = 1.88$  in the case of natural abundant of isotopes where 75% are even. The second spectrum obtained after co-implantation of  $^{95}Mo(I=5/2)$  and  $O^+$  the axial spectrum with HFS is observed (Fig 6). This spectrum is described by spin Hamiltonian (1).

Computer simulation of EPR spectrum of  $50CaO-50 P_2O_5$  implanted with  $^{95}Mo^+$  to fluence  $F = 5 \times 10^{16} \text{ cm}^{-2}$  presented in Figure 6 shows that the best – fit parameters are  $g_{\parallel} = 1.900 \pm 0.002$ ;  $g_{\perp} = 1.925 \pm 0.005$ ;  $A_{\parallel} = (89 \pm 3) \times 10^{-4} \text{ cm}^{-1}$  and  $A_{\perp} = (49 \pm 3) \times 10^{-4} \text{ cm}^{-1}$ .

## CONCLUSION

1. The analysis of EPR and optical data obtained in the present work as well as in Ref. [7,14] shows that the ions of transition metals  $Ti^{3+}$ ,  $V^{3+}$ ,  $V^{4+}$ ,  $Cr^{3+}$ ,  $Mn^{2+}$ ,  $Co^{2+}$ ,  $Cu^{2+}$ ,  $Mo^{5+}$  can be present in isolated states in implantation layers of phosphate glasses at a rather low fluences ( $\leq 5 \times 10^{16} \text{ cm}^{-2}$ ). The ions in high valence forms ( $V^{4+}$ ,  $Mo^{5+}$ ) are formed only in the case of co-implantation with  $O^+$ .

2. The ions  $Ti^{3+}$ ,  $V^{4+}$ ,  $Mo^{5+}$  are in tetragonally compressed octahedral and ion  $Cu^{2+}$  in tetragonally elongated octahedron, i. e. are in their the most typical environments. However, spectral of corresponding composition melted from the batch.
3. At high fluences ( $\geq 10^{17} cm^{-2}$ ) some TM ions can form in implanted phosphate glasses compounds with O or PO groups (for example,  $MnO$ ,  $VO_2$ ,  $CrO_2$ ,  $Ti_xPO_4$ ).

## REFERENCES

1. **G. W. Arnold, P. Mazzoldi**, Ion Beam Modification of Glasses, in: *Ion Beam Modification of Insulators*, ed. P. Mazzoldi and G. W. Arnold (Elsevier, Amsterdam, 1987), Ch. 5, pp 195-222.
2. **H. Hosono, Y. Ikuhara, Y. Abe, R. A. Weeks**, *J. Mater. Sci. Lett.* 11, 1257 (1992)
3. **G. Wichard, R. A. Weeks, R. A. Zuhr**, in: *Proc. 15<sup>th</sup> Intern. Congress. On Glass. Leningrad, 1989*. ed. O. V. Mazurin, Vol. 2b (Nauka, Leningrad), 271
4. **H. Hosono and R. A. Weeks**, *Phys. Rev.* B40, 10543 (1989).
5. **G. Wichard, H. Hosono, R. A. Weeks, R. A. Zuhr and R. H. Magruder**, *J. Appl. Phys.*, 67, 7526 (1990)
6. **L. D. Bogomolova**, *Short Abstracts, Second Int. Conf. On Silica Sci and Techn. "SILICA 2001"*, Mulhouse, France, 3-6 Sept. 2001, 225.
7. **Abukais, L. D. Bogomolova, A.A. Deshkovlaskaya, V. A. Jachkin, N. A. Krasil'nikova, S. A. Prushinsky, O. A. Trul. S. V. Stefanovsky, E. A. Jilinskaya**, *Optical Materials*, 18, 295 (2002).
8. **Aboukaïs, L. D. Bogomolova, E. Cattaruzza, A. A. Deshkovskaya, N. A. Krasil'nikova, S. A. Prushinsky, E. A. Zhinlinskaya**, *Optical Materials* (in press)
9. **L. D. Bogomolova, Yu. G. Tepliyakov, F. Caccavale**, *J. Non-Crystal. Solids*, 194, 291 (1996)
10. **L. D. Bogomolova, V. A. Jachkin, S. A. Prushinsky, S. A. Dmitriev, S. V. Stefanovsky, Yu. G. Tepliyakov, F. Caccavale, E. Cattaruzza, R. Bertonello, F. Trivillin**. *J. Non-Crystal. Solids*, 210, 101 (1997)
11. **L. D. Bogomolova, V. A. Jachkin, S. A. Prushinsky, S. V. Stefanovsky, Yu. G. Tepliyakov, F. Caccavale**, *J. Non-Crystal; Solids*, 220, 109 (1997)
12. **L. D. Bogomolova, V. A. Jachkin, S. A. Prushinsky, S. A. Dmitriev, S. V. Stefanovsky, Yu. G. Tepliyakov, F. Caccavale**, *J. Non-Crystal; Solids*, 241, 174 (1998)
13. **L. D. Bogomolova, A. A. Deshkovskaya, N. A. Krasil'nikova, G. BataV. A. Jachkin, S. A. Prushinsky, S. V. Stefanovsky, Yu. G. Tepliyakov, F. Caccavale**, *J. Non-Crystal; Solids*, 220, 109 (1997)
14. **L. Bogomolova, S, P, Prushinsky, N. Krasil'nikova, O. Trul, S. Stefanovsky**, *Phys. Chem. Glasses*, 43C, 25 (2002)
15. **L. D. Bogomolova, A. N. Khabarova, E. V. Klimashina, N. A. Krasil'nikova, V. F. Jachkin**, *J. Non-Crystal. Solids*, 103, 319 (1988)
16. **S. Arafa, A. Byshay**, *Phys. Chem. Glasses*, 1, 1105 (1970)
17. **D. L. Griscom**, *J. Non-Crystalline Solids*, 40, 211 (1980)
18. **N. R. Yafaev, Yu. V. Yablokov**, *Sov. Phys. Solid. State*, 4, 1123 (1962)
19. **Paul, G. C. Upreti**, *J. Mater Sci.* 10, 692 (1975)
20. **V. K. Zakharov, D. M. Yudin**, *Sov. Phys.-Solid St.*, 7, 1267 (1965)
21. **R. J. Landry, J. T. Fournier, C. G. Young**, *J. Chem. Phys.* 46, 1285 (1967)
22. **S. Kumar**, *Phys. Chem. Glasses*, 5, 107 (1964)
23. **L. D. Bogomolova, V. A. Jachkin, V. N. Lazukin, T. K. Pavlushkina, V. A. Shmuckler, J. Non-Crystal. Solids**, 28,375 (1978)

24. **L. D. Bogomolova, T. K. Pavlushkina, A. V. Roshchina**, *J. Non-Crystal. Solids*, 58,99 (1983)
25. **V. Cristea, A. Goldstein**, *Mater de Constr.*, V, 15 (1985) (in Roman)
26. **G. Shpe'rlich, G. Frank, W. Rhein**, *Phys. Status Solidi*, 54, 241 (1972)
27. **N. Kinomura, F. Muto, M. Koismi**, *J. Solid State Chem.* 45, 252 (1982)
28. **D. L. Griscom**. *J. Non-Crystalline Solids*, 42, 287 (1980)
29. **L. Chamberland**, *CRC Crit. Rev. Solid. State Mater, Sci.* 7, 1 (1977)
30. **K. Köhler, W. Mörke, T. Bieruta**, *Colloids and Surfaces A: Physicochem. And Eng. Aspects*, 144, 87 (1998)
31. **H. Hosono, H. Kawazoe, T. Kanazawa**, *J. Non-Crystalline Solids*, 37, 427 (1980)
32. **W. Low** "Paramagnetic resonance in Solids", Academic press, NY and London, 1960, pp, 240
33. **S. Ruck, D. Stachel**, *Phosphorus Research Bul.* 13, 201 (2002)
34. **L. D. Bogomolova, V. N. Lazukin, N. V. Petrovykh**, *DAN SSSR*, 181, 313 (1968)
35. **J. Matsuda, K. Kojima, H. Yano, H. Marusawa**, *J. Non-Crystal Solids*. 111, 63 (1989)
36. **K. Kojima, H. Yanj, J. Matsuda**, *J. Amer. Ceram. Soc.* 232, 134 (1990)